COMPUTER GRAPHICS AND IMAGE PROCESSING 10, 95–114 (1979)

Random Pattern Generation Processes*

BRUCE SCHACHTER

General Electric Co., P.O. Box 2500, Room 4324, Daytona Beach, Florida 32015

AND

NARENDRA AHUJA

University of Maryland Computer Science Center, Computer Vision Laboratory, College Park, Maryland 20742

Received August 2, 1978

This paper describes some geometric processes giving rise to patterns that may be useful for image modelling. Some properties of these processes are described. Several statistics are suggested for modelling purposes. Examples of the patterns that can be generated in this way are provided.

1. INTRODUCTION

This paper deals with a new class of image models called mosaic models that view an image as a random pattern and model it by an appropriate planar process. There are several different kinds of image models in use. Mandelbrot [1] models irregular and fragmentary natural patterns by Brownian surfaces (Fig. 1). Wong [2], Hassner [3], and others model images by two-dimensional random fields. Matheron [4] and a number of other French mathematicians describe random spatial patterns in terms of regionalized random variables. McCormick and Jayaramamurthy [5] and others use time series analysis to model the row-scan of the image.

In this paper we provide an overview of a variety of mosaic models. Subsequent papers will discuss their specific properties and their applications to images.

We describe a number of models for spatial point patterns in Section 2. The "most random" of these, the Poisson point process, will be used in the construction of most of the succeeding patterns.

In Section 3, we will model piecewise contiguous patterns by random mosaics. The use of mosaics to depict patterns is ancient. The Chaldeans were skilled mosaicists by 2500 BCE. The Greeks further developed the art and were thought to have used pattern books for standard motifs. The pieces of a mosaic were

* The authors wish to thank Azriel Rosenfeld and Durga Panda for many helpful discussions. The support of the U.S. Air Force Office of Scientific Research under Grant AFOSR-77-3271 is gratefully acknowledged.

0146-664X/79/060095-20$02.00/0

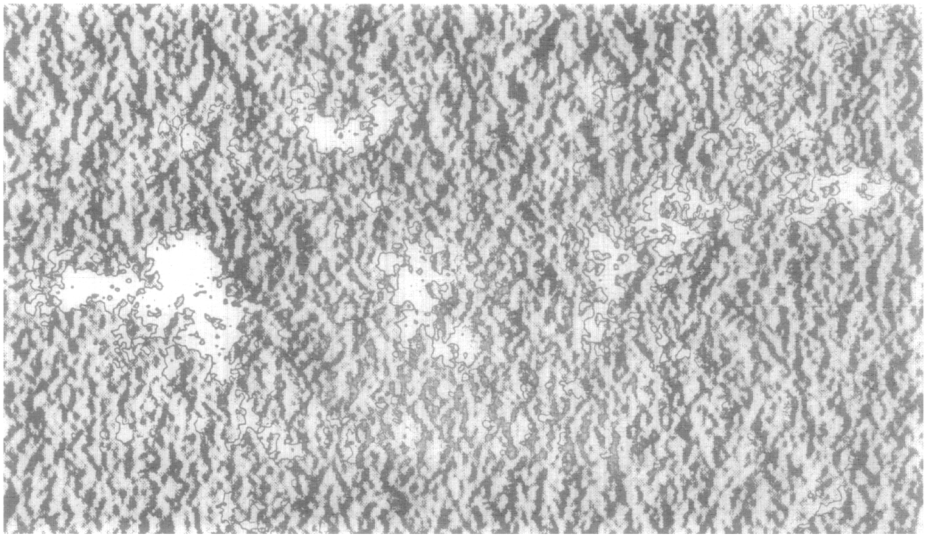

FIG. 1. Brownian surface texture [1].

known to the Romans as tesserae or tessellae. A mosaic having a simple geometric design was known as opus tesselatum—giving rise to the current term "tessellation." One of the mosaic models, the Poisson line model, has interesting Markovian properties. Another, the occupancy model, mimics natural cell growth processes.

We will discuss bombing models in Section 4. The bombs are geometric figures that are dropped onto a plane. These figures in union are the foreground of a pattern, with the uncovered portion of the plane forming the background. Many natural two-color patterns are formed by bombing processes or at least can be modeled by them; e.g., bubble holes on the surface of cement, leaves on the ground, pebbles on a beach, small stones on the surface of asphalt, etc.

Some statistical properties of our models will be noted in Section 5. Finally, in Section 6, we will suggest projects for future research. We also show computer-generated examples of patterns produced by all the primary models covered in Sections 2 through 4.

2. POINT PROCESSES

Each realization of a two-dimensional point process is a countable set of points in the plane R^2. The important random variables characterizing the process are the $Z(A)$, which count the number of points within each Borel set $A \subset R^2$. If A is bounded, then $Z(A)$ must be finite. We will assume that $E[Z(A)^2]$ is also finite.

The simplest parameter of this process is its intensity $\lambda = E[Z(A)]$. The second-order statistics of the process may be reduced to a function $K \in (0, \infty)$. Ripley [6] gives the following intuitive definitions of K.

(i) $\lambda^2 K(t)$ is the expected number of ordered pairs of distinct points less than t apart, with the first point within a given region of unit area.

(ii) $\lambda K(t)$ is the expected number of further points within t of an arbitrary point of the process.

(iii) Under additional assumptions $g(t) = (\lambda^2/2\pi t)(dK/dt)$ is a joint density for the occurrence of two points distance t apart.

We will give several examples of two-dimensional point processes. Only the first of these will be used in the generation of the patterns discussed in the remaining sections of this paper.

(1) Two-dimensional Poisson Point Process

This process is completely characterized by the properties that the expected number of points within a region of area A is λA, irrespective of the shape or orientation of the region; and that the numbers of points in any two disjoint regions are independent. For this model $K(t) = \pi t^2$. On a grid the Poisson process becomes a binomial process [24]. Each grid point has a probability $1 - e^{-\lambda}$ of being dropped by the process (Fig. 2). These points can be thought of as dropped onto the square, like raindrops falling on a puddle, or meteorites striking the moon.

Not all point patterns are so random, i.e., a point's nearest neighbors may be closer or farther than predicted under a Poisson model. Models which produce clustered point patterns will have $K(t) > \pi t^2$, whereas models yielding inhibitory point patterns will have $K(t) < \pi t^2$.

(2) Clustering Model (Center-Satellite Process)

Particles are parents (or nuclei) of families of children (satellites). The parents may be dispersed in a Poisson manner with their children congregating about them.

One example is the Neyman–Scott process. The daughter process is a random number N of independently distributed points. The parent process is Poisson of intensity α. Here $\lambda = \alpha E[N]$. The probability density of the distribution of the distance between two arbitrary points of the dughter process is given by $f(t)$, yielding [6]

$$g(t) = \lambda^2 + \alpha E\{N(N-1)\} f(t)/2\pi t.$$

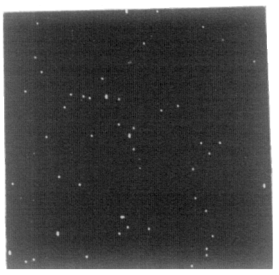

FIG. 2. A realization of a two-dimensional Poisson point process.

(3) Inhibitory Model

Particles appear to repel their neighbors, as if they were animals defending their territory. One example of an inhibitory model is given by Matern [7]. We examine a two-dimensional Poisson point process of intensity α and delete any point that is within distance $2d$ of another point. For this process

$$\lambda = \exp(-4\pi\alpha d^2); \qquad g(t) = 0; \qquad t \leq 2d$$
$$= \lambda^2 \exp(-\alpha U(t)); \qquad t > 2d,$$

where $U(t)$ is the area covered by two circles each of radius d, centered at distance t apart.

(4) Other Models

Many other categories of two-dimensional point processes are discussed in the statistics literature. For example, we may vary a process's intensity temporally to produce a space-time point process. Other classes have been proposed which are mixtures of simpler models. The most notable of these are the mixed Poisson and doubly stochastic [8] Poisson models. Other models, such as Markov and diffusion processes, have also been used to describe certain point patterns. For a good overview of the subject see Ripley [6, 9] and Bartlett [10].

3. CELL STRUCTURE MODELS

Random mosaics are constructed in two steps:

(1) Tessellate a planar region into cells. We will only consider tessellations composed of bounded convex polygons.

(2) Independently assign one of m colors to each cell according to a fixed set of probabilities

$$p_1, \ldots, p_m; \sum_{i=1}^{m} p_i = 1.^1$$

By this process, we partition region A into subregions $A_1, \ldots, A_m$; $\bigcup^m{}_{j=1} A_j = A$, where A_j is defined to be the union of all cells of color j. The partitioning of A is the realization of a random process with the following stationary and transition probabilities:

(1) For all $s \in A$, Pr $(s \in A_i) = p_i$ for $i = 1, 2, \ldots, m$.

(2) For all $(s, s') \in A$, with distance $d = |s - s'|$ between them,
$$\Pr(s' \in A_i | s \in A_j) = P_{ij}(d) = p_i(1 - W(d)) + \delta_{ij} W(d)$$

for $i, j = 1, 2, \ldots, m$. $W(d)$ is the probability that any two points that are distance d apart are both in the same cell, and δ_{ij} is the Kronecker delta.

Cell structure models form a family whose members differ only in the manner in which the plane is tessellated. We will describe some important members of

[1] Other random coloring schemes are possible. Examples: (i) Each cell has a constant color throughout, where the constants are independently chosen from a single normal distribution. (ii) All cell borders are given a thickness and one color, and all cell interiors are given a second color.

this family, starting with the most random members and progressing toward more regular examples.

The first model we will consider is a *Gaussian random process*. It is a degenerate form of a cell structure model, in that each point of an image constitutes an entire cell.

Nondegenerate cell structure models are constructed by two types of processes: (1) line processes and (2) cell growth processes. The first type of process uses straight lines to partition a region into cells. The positions and orientations of these lines can range from randomly distributed (*Poisson line model*) to regularly arranged (*checkerboard model*). The second type of process uses a spatial point process to generate the nuclei of growing cells. If the nuclei are randomly positioned an *occupancy model* is produced.

3.1. Gaussian Random Process

A real random vector process $\{Y_{s_i} | s_i \in A\}$ is a Gaussian random process if for every finite set of points $\{s_i\} \in A$, the corresponding random vectors Y_{s_i} are jointly Gaussian random vectors. A (stationary) Gaussian random vector process is completely defined (statistically) by its mean $\mu = E(Y_{s_i})$ and auto-covariance matrix $\Sigma(b)$, where $\Sigma(b) = E[(Y_{s_{i+b}} - \mu)(Y_{s_i} - \mu)^t]$. The process reduces to one of white noise if $\Sigma(b) = \Sigma(0) \cdot \Delta(b)$, where $\Delta(b) = 1$ when $b = 0$, and $\Delta(b) = 0$ otherwise.

3.2. Random Line and Cell Growth Processes

(*a*) *Poisson Line Model:* $\mathfrak{L}(\lambda, p_1, \ldots, p_{m-1}, \mu_1, \ldots, \mu_m, \Sigma_1, \ldots, \Sigma_m)$. Consider a system of intersecting lines in the plane with random positions and orientations. Such a system when derived by the following Poisson process possesses fundamental properties of homogeneity and isotropy. A Poisson process of intensity λ chooses points (θ, p) in the infinite rectangular strip $[0 \leq \theta < \pi, -\infty < p < \infty]$. Each of these points can be used to construct a line in the plane of the form $x \cos\theta + y \sin\theta - p = 0$, where p is the distance to an arbitrarily chosen origin. One can use this process to tessellate any finite region A into cells (Fig. 3a). It can be seen that there are almost certainly four cells converging at each vertex. These cells are then colored in the manner previously described.

The sequence of colors obtained by sampling an m-color Poisson line mosaic at equal intervals is an m-state discrete Markov chain with transition matrix $P(d)$ given by

$$P(d) = \begin{array}{c} \\ A_1 \\ A_2 \\ \vdots \\ A_m \end{array} \begin{array}{c} \begin{array}{cccc} A_1 & A_2 & \cdots & A_m \end{array} \\ \begin{bmatrix} P_{11}(d) & P_{21}(d) & \cdots & P_{m1}(d) \\ P_{12}(d) & P_{22}(d) & \cdots & P_{m2}(d) \\ \vdots & \vdots & & \vdots \\ P_{1m}(d) & P_{2m}(d) & \cdots & P_{mm}(d) \end{bmatrix} \end{array},$$

where d is the sampling interval. A matrix of the above form is a necessary but not sufficient condition for randomness. The additional requirement for the random mingling of the color cells places a further restriction on $P(d)$; namely

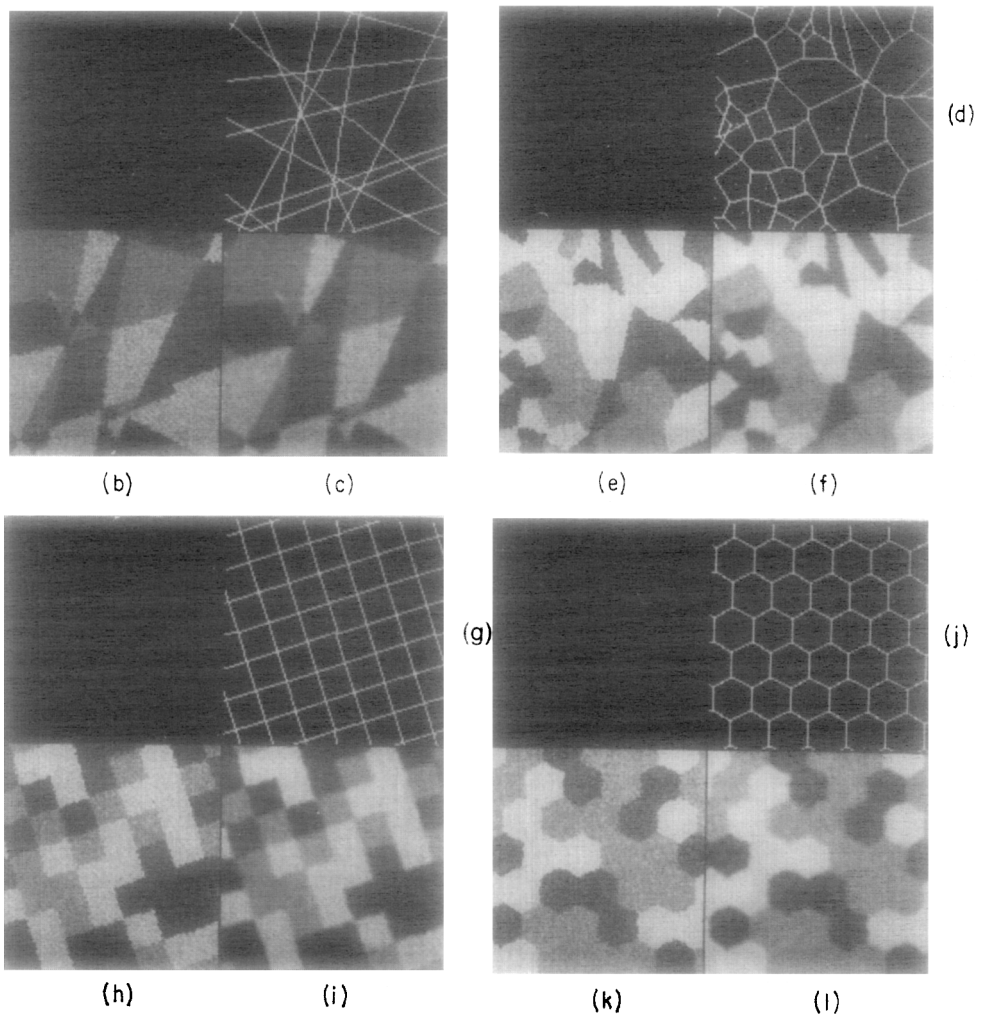

FIG. 3. Cell structure models. (a) Poisson line tessellation, (b) $\mathfrak{L}(16, (.33, .33, .34), (15, 30, 45), (25, 25, 25))$ (c) $2b$ mean filtered over a 3-by-3 neighborhood, (d) Occupancy model tessellation, (e) $\mathfrak{O}(40, (.33, .33, .34), (15, 30, 45), (25, 25, 25))$, (f) $2e$ mean filtered over a 3-by-3 neighborhood, (g) Rotated checkerboard tessellation, (h) $\mathfrak{C}(10/127, (.33, .33, .34), (15, 30, 50), (25, 25, 25))$, (i) $2h$ mean filtered over a 3-by-3 neighborhood, (j) Rotated hexagonal tessellation, (k) $\mathfrak{IC}(40, (.33, .33, .34), (15, 30, 45), (25, 25, 25))$, (l) $2.k$ mean filtered over a 3-by-3 neighborhood.

$P_{j\alpha} = P_{j\beta}$ for all $\alpha, \beta \neq j$. A Markov transition matrix having this form possesses the following properties [11, 12]:

(1) Reversibility—The probability that color region A_i follows A_j in the sampling sequence is the same as the probability that A_j follows A_i. This condition can be expressed in terms of the stationary and transition probabilities of the process

$$p_j P_{ij}(d) = p_i P_{ji}(d), \qquad \text{where } P_{ij}(d) = p_i(1 - W(d)) + \delta_{ij} W(d) \quad \text{and } W(d) = e^{-2\lambda d}. \quad (1)$$

There are many situations when a texture does not possess this property. For example, consider an aerial photograph of a field where the distribution of plant species is controlled by the prevailing winds or predominant direction of sunlight.

(2) Lumpability—The chain resulting from any regrouping or renaming of the color states is still Markov.

(3) Specifiability—A random m-color Poisson line mosaic is completely specified by $3m$ parameters. To specify the area covered by each of the colors we need to provide any $m - 1$ independent terms of the stationary probability vector $(p_1, p_2, \ldots, p_m)$. To specify the transition matrix we need P_{ij} for all i and j. However, the form of Eq. (1) indicates that the entire matrix can be specified by the stationary probability vector and only one other parameter. That parameter is λ, the intensity of the driving point process.

An additional $2m$ parameters are needed for the means and covariances of the m colors.

(4) The chain is irreducible, aperiodic, and all its states are recurrent states, since $0 < P_{ij}(d) < 1$ for all i and j. These properties are defined as follows. The period of state α of a Markov chian is the greatest common divisor of all integers $n \geq 1$ for which the probability of returning to state α, starting from state α, in n steps is nonzero. A Markov chain is aperiodic if its period is 1. A Markov chain is irreducible if all its states are accessible from each other. A state of a Markov chain is recurrent if when we start from the state we will eventually return to it.

Two or more contiguous cells of the same color are said to form a patch. We would next like to derive the ratio of patch width to cell width. Consider the distribution of length l_α of color α along a transect. It can be shown [11] that the sizes of neighboring cells are independent for a Poisson line tessellation. The points of intersection of an arbitrary line with a Poisson line tessellation constitute a Poisson line process with intensity 2λ. This means that the expected number k of lines crossing a transect of unit length is 2λ. Thus l_α is the sum of j independent values of $1/k$. Let $g(l_\alpha \mid j)$ denote the conditional pdf of l_α given j. Then

$$g(l_\alpha \mid j) = \frac{(2\lambda)^j l_\alpha{}^{j-1} e^{-(2\lambda)}}{(j-1)!}.$$

A run of j cells of color α will occur if the succeeding $j - 1$ cells are of color α and a cell of another color follows to terminate the run. The probability that this will happen is $p_\alpha{}^{j-1}(1 - p_\alpha)$. The conditional pdf of l_α when j is allowed to vary is therefore

$$\begin{aligned} g(l_\alpha) &= \sum_{j=1}^{\infty} g(l_\alpha \mid j) p_\alpha{}^{j-1}(1 - p_\alpha) \\ &= 2\lambda(1 - p_\alpha) e^{-2\lambda l_\alpha} \sum_{j=1}^{\infty} \frac{(2\lambda p_\alpha l_\alpha)^{j-1}}{(j-1)!} \\ &= 2\lambda(1 - p_\alpha) e^{-2\lambda l_\alpha (1 - p_\alpha)}. \end{aligned}$$

Thus the expected width of a patch of color α is $1/(1 - p_\alpha)$ times the expected cell width.

Showing that a texture fits a Poisson line model requires the proof of a very complicated hypothesis. We must show that (i) the pattern is not directionally dependent, (ii) cells of all colors are randomly mingled, and (iii) the pattern of each color when taken against a background of the remaining colors forms a 2-color Poisson line mosaic.

(*b*) *Occupancy Model:* $\mathcal{O}(\lambda, p_1, \ldots, p_{m-1}, \mu, \ldots, \mu_m, \Sigma_1, \ldots, \Sigma_m)$. The occupancy model is defined as follows. A Poisson process with intensity λ drops points onto the plane. Each of these points spreads out to occupy a "Dirichlet cell" consisting of all points on the plane that are nearer to it than to any of the other Poisson points. These cells are convex Voronoi polygons having, on the average, six sides (Fig. 3d). (It can be shown that nearest neighbors can be determined in $\mathcal{O}(\lambda \log \lambda)$ time.) These cells are then independently assigned colors as usual.

Matern [7] has derived $W(d)$ for the occupancy model as a very complex double integral having no elementary solution.

Two models that are related to the occupancy model will be briefly noted. A random triangular tessellation can be constructed from *Delaunay triangles* [13] that have as their vertices the three nuclei that are equidistant from a vertex of a Voronoi polygon. Thus the intersections of the borders of Voronoi polygons are the circumcenters of the Delaunay triangles (see Fig. 4).

The *Johnson–Mehl model* [14] is often used to describe metallurgical surfaces. This model differs from the occupancy model only in that points are dropped onto the plane as a function of time; i.e., $\lambda = \lambda(\tau)$. These points start expanding circularly as soon as they hit the plane. A point on the plane is assigned to the cell whose expanding border first reaches it. Cells formed by this process do not have straight line edges and are not necessarily convex (Fig. 5). Irregular configurations occur when late arriving points fall near the interface of two large cells.

The occupancy model simulates natural growth processes in the plane. In contrast, Poisson line mosaics are surely less common. The cells of most natural textures do not have the sharp corners of a Poisson line cell (two exceptions are blades of grass and the leaves of a palm tree).

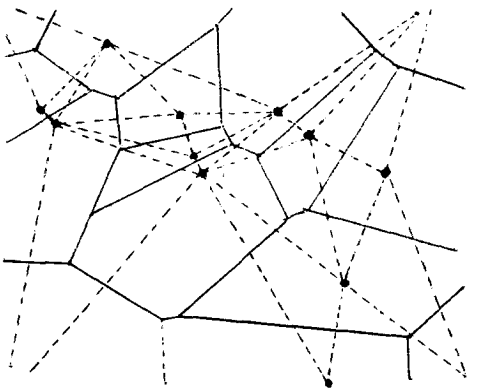

FIG. 4. Cells generated by occupancy model. Delaunay triangles shown as dashed lines.

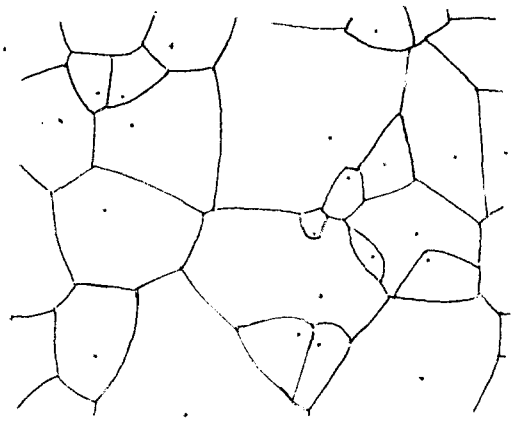

FIG. 5. Cells generated by the Johnson–Mehl model [14].

Despite its "unnatural" appearence, the Poisson line model may be suggested as a texture standard because of its randomness. For example, it is the only texture which meets the requirements for Markovianity in the plane; the sizes of its adjacent cells are independent [11], and its correlation function has an exponential form [12]. The occupancy model does not satisfy either of these conditions.

3.3. Regular Line and Cell Growth Processes

(*a*) *Rotated Checkerboard Model:* $C(b, p_1, \ldots, p_{m-1}, \mu_1, \ldots, \mu_m, \Sigma_1, \ldots, \Sigma_m)$. This is an example of a cell structure model where the cells have a uniform diameter. A checkerboard model can be formed by the following procedure. First choose the origin of an x–y coordinate system on the plane with uniform probability density. Then tessellate the plane into square cells of side length b. Next, this "checkerboard" is rotated by an angle chosen with uniform probability from the interval $(0, 2\pi)$. The cells are now independently assigned one of the m tile types as before (Fig. 3h). The solution for $W(d)$ for this model is discussed in the statistics literature as an extension of Buffon's needle problem:

$$W(d) = 1 - 4d/\pi b + d^2/\pi b^2 \qquad (d \leq b)$$

$$= 1 - 2/\pi - (4/\pi)\cos^{-1}(b/d) - d^2/\pi b^2 + (4/\pi)(d^2/b^2 - 1)^{\frac{1}{2}} \qquad (b < d \leq 2^{\frac{1}{2}}b)$$

$$= 0 \qquad (d > 2^{\frac{1}{2}}b).$$

(*b*) *Rotated Hexagon Model* [15]: $H(\lambda, p_1, \ldots, p_{m-1}, \mu_1, \ldots, \mu_m, \Sigma_1, \ldots, \Sigma_m)$. This model is analogous to the checkerboard model, except that hexagons are used in place of squares. Another way of viewing these models is as follows: Consider a system of particles on the vertices of a regular lattice (Figs. 6 and 7a). Let these particles be the nuclei of growing cells. Cells will grow unimpeded in a circular fashion until they reach the tightly packed state shown in Figs. 6 and 7b.

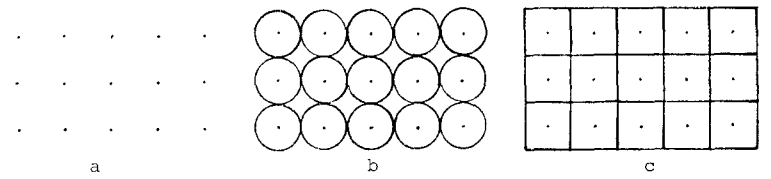

FIG. 6. Square growth process.

At this moment each circle has four or six points of contact with its neighbors, depending on the nature of the lattice. As the cells continue to grow these points of contact will be extended into lines, and the equal circles shown in Figs. 6 and 7b will be converted into the equal hexagons or squares shown in Figs. 6 and 7c. For hexagons of side length a, $W(d)$ can be derived from equations given by Santaló [16] and Matern [7]

$$W(d) = 1 - \frac{4(3)^{\frac{1}{2}}d}{3\pi a} + \left(\frac{3^{\frac{1}{2}}}{3\pi} - \frac{1}{9}\right)\left(\frac{d}{a}\right)^2 \qquad \text{for } d \leq a$$

$$= \frac{5 + (d/a)^2}{3} - \frac{1}{\pi}\left(12\left(\frac{d}{a}\right)^2 + 9\right)^{\frac{1}{2}} - \left[\frac{4}{3\pi}\left(\frac{d}{a}\right)^2 + \frac{2}{\pi}\right]\sin^{-1}\left[\frac{3^{\frac{1}{2}}}{2}\left(\frac{d}{a}\right)^2\right]$$

$$\text{for } a < d \leq 3^{\frac{1}{2}}a$$

$$= \left(\frac{2}{3\pi}\left(\frac{d}{a}\right)^2 + \frac{8}{\pi}\right)\left[\sin^{-1}\left(\frac{3^{\frac{1}{2}}a}{d}\right) - \frac{\pi}{3}\right] - \frac{3^{\frac{1}{2}}}{3\pi}\left[\left(\frac{d}{a}\right)^2 + 6\right]$$

$$+ \frac{10}{3\pi}\left(3\left(\frac{d}{a}\right)^2 - 9\right)^{\frac{1}{2}} \qquad \text{for } 3^{\frac{1}{2}}a < d \leq 2a$$

$$= 0 \qquad \text{for } d > 2a.$$

(c) *Rotated Triangular Model:* $\mathcal{T}(b, p_1, \ldots, p_{m-1}, \mu_1, \ldots, \mu_m, \Sigma_1, \ldots, \Sigma_m)$. An equilateral triangular tessellation can be formed by connecting the growth centers of neighboring cells in a hexagonal tessellation (Fig. 8). For triangles of side length b, $W(d)$ can be derived from equations given by Santaló [16] and Matern [7]

$$W(d) = W_1(d) + W_2(d),$$

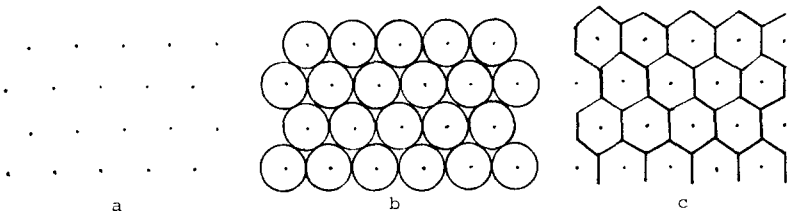

FIG. 7. Hexagonal growth process.

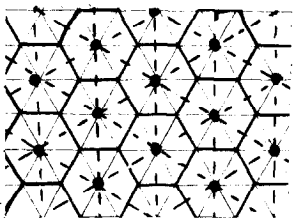

FIG. 8. Hexagonal tessellation.

where

$$W_1(d) = 1 - \frac{4(3)^{\frac{1}{2}}d}{\pi b} + 2\left(\frac{3^{\frac{1}{2}}}{2\pi} + \frac{1}{3}\right)\left(\frac{d}{b}\right)^2 \qquad \text{for } d \leq b$$

$$= 0 \qquad \text{otherwise,}$$

$$W_2(d) = \frac{3}{\pi}\left[12\left(\frac{d}{b}\right)^2 - 9\right]^{\frac{1}{2}} + \frac{2}{\pi}\left[2\left(\frac{d}{b}\right)^2 + 3\right]\cos^{-1}\left(\frac{3^{\frac{1}{2}}b}{2d}\right) \qquad \text{for } \frac{3^{\frac{1}{2}}b}{2} \leq d \leq b$$

$$= 0 \qquad \text{otherwise.}$$

4. BOMBING MODELS

Random two-color patterns can be formed by bombing processes. The bombs are geometric figures that are dropped onto the plane. The sizes and shapes of these figures are fixed, but their positions and orientations are random. The location of a figure is determined by its center point (x_0, y_0) (i.e., center of gravity), and the orientation θ of its principal axis. By this process a fixed region A is randomly partitioned into A_1 and $A_2 = \{A - A_1\}$, where A_1 consists of that part of A that is covered by the dropped figures. We shall refer to the figures comprising A_1 as isotropically distributed.

We are assuming translation invariance. Hence the number of center points falling on any subregion of the plane depends only upon the area of the subregion—not on its shape or orientation. The number of center points falling on any subregion A has a Poisson distribution with mean λA, where λ is the expected number of center points falling on any unit area of the plane.

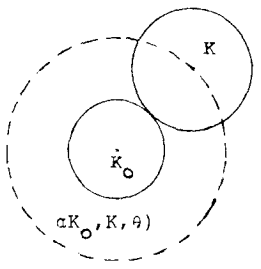

FIG. 9. $\alpha(K_0, K, \theta)$ for two circles.

To complete the specification of our model, we will color regions A_1 and A_2 in a Gaussian fashion, with distributions $N(\mu_1, \Sigma_1)$ and $N(\mu_2, \Sigma_2)$, respectively. We will now consider three coverage theorems for bombing processes.

Let K be a randomly positioned convex figure with fixed orientation θ. Let K_0 be another convex region. Let $\alpha(K_0, K, \theta)$ denote the area in which the center point of K can be placed so that K intersects K_0. The area $\alpha(K_0, K, \theta)$ has as its border the locus of points where the center point of K might fall so that the region K with orientation θ just touches the borders of K_0 (Fig. 9).

The measure of all center points of the figure K where it intersects K_0 is

$$m(K_0, K) = \int_0^{2\pi} \alpha(K_0, K, \theta) dF\theta,$$

where $F(\theta)$ is the distribution function of the orientation parameter θ.

THEOREM I (Dufour [17]). *Consider an infinite collection of congruent convex figures K independently, identically, and homogeneously distributed over the plane. The number of figures K intersecting another convex figure K_0 has a Poisson distribution with mean $\lambda m(K_0, K)$.*

THEOREM II (Dufour [17]). *Consider an infinite collection of congruent convex figures of area a and perimeter L distributed isotropically, independently, and homogeneously throughout the plane. The number of such figures intersecting another convex figure of area a_0 and perimeter L_0 has a Poisson distribution with mean $\lambda(a_0 + a + L_0 L/2\pi)$.*

Consider a circular bombing process of intensity λ. For a circle of radius r, the probability p_2 that a point chosen at random on the plane is isolated is equal to the probability that there is no circle within a radius r around the point as its center. Thus $p_2 = \exp(-\pi r^2\lambda) = \exp(-\lambda\alpha)$, where α is the area of a circle. The proportion p_1 of the plane covered by circles is the probability that a point is not isolated: $p_1 = 1 - p_2 = 1 - \exp(-\lambda\alpha)$. Notice that if we drop two circles of area $\frac{1}{2}\alpha$ every time we previously dropped a single circle, the area covered will be unchanged. The fact that two small circles cannot possibly combine to produce the same shape as a single larger circle suggests that the area covered is independent of the shape of the dropped figures.

THEOREM III. *If an infinite collection of congruent convex figures, each of area α, are isotropically, independently, and homogeneously distributed throughout the plane, then the proportion p_1 of the plane covered by the figures is $1 - \exp(-\lambda\alpha)$.*

Proof. This follows directly from Theorem I. Let K_0 be a point on the plane. The number N of randomly dropped figures K intersecting the point K_0 has a Poisson distribution with mean $\lambda\alpha$, where α is the area of K. Therefore

$$f(N) = \frac{1}{N!}(\lambda\alpha)^N e^{-\lambda\alpha}.$$

The probability p_2 that a point is isolated is the probability that $N = 0$

$$p_2 = \Pr(N = 0) = f(0) = e^{-\lambda\alpha}.$$

The probability p_1 that a point is not isolated is therefore $1 - e^{-\lambda\alpha}$.

Theorem III relates the number of dropped figures to the proportion of the plane covered

$$\lambda = \frac{-1}{\alpha} \ln (1 - p_1) = -\frac{1}{\alpha} \ln p_2.$$

This is a useful equation for estimating the number of particles on a microscope slide, parts on a conveyor belt, trees in a field, etc.

Examples of Bombing Processes

(*a*) *Random Line Segment Processes:* $\mathcal{L}(\tau, l)$. Line segments each of length l are distributed isotropically over the plane. The orientation of a line segment is specified by the angle θ between the x-axis and the perpendicular to the line segment. The midpoint (x_0, y_0) of the line segment specifies its position.

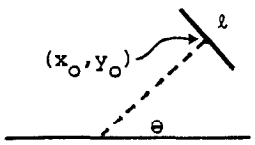

Assume that we are given two line segments centered at randomly selected points P and Q, with an angle θ between them. They will intersect if P falls within a rhombus of side length l centered at Q.

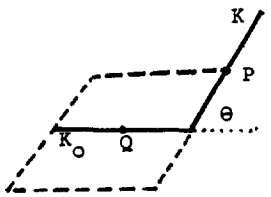

The area of the rhombus is $l^2 \sin\theta$, so that we have

$$m(K_0, K) = 2\int_0^{\pi} \tfrac{1}{2} l^2 \sin\theta dF\theta = 2\int_0^{\pi} \frac{l^2}{2\pi} \sin\theta d\theta = \frac{2l^2}{\pi}.$$

Thus from Theorem I, the number N of randomly distributed line segments of length l intersecting a fixed line segment of length l has a Poisson distribution with mean $2\lambda l^2/\pi$,

$$f(N) = \frac{1}{N!}\left(\frac{2\lambda l^2}{\pi}\right)^N \exp\left(\frac{-2\lambda l^2}{\pi}\right).$$

The probability p_0 that a line segment is isolated is the probability that N is zero.

$$p_0 = \Pr(N = 0) = f(0) = \exp(-2\lambda l^2/\pi).$$

(*b*) *Elliptical Bombing Process.* $\mathcal{E}(\lambda, c_1, c_2, \mu_1, \Sigma_1, \mu_2, \Sigma_2)$. Ellipses having major axis $2c_1$ and minor axis $2c_2$ are distributed randomly over the plane. The orientation of an ellipse is specified by the angle θ between the x-axis and the perpendicular to the major axis of the ellipse. The midpoint of the ellipse specifies its position.

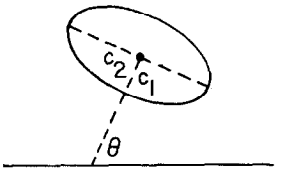

The parametric equations for the ellipse are

$$x - x_0 = c_1 \cos\alpha \cos\theta - c_2 \sin\alpha \sin\theta,$$
$$y - y_0 = c_1 \cos\alpha \sin\theta + c_2 \sin\alpha \cos\theta;$$

where α is between 0 and 2π. Thus

$$\frac{(x - x_0)}{c_1}\cos\theta + \frac{(y - y_0)}{c_1}\sin\theta = \cos\alpha,$$
$$\frac{-(x - x_0)}{c_2}\sin\theta + \frac{(y - y_0)}{c_2}\cos\theta = \sin\alpha.$$

The equation for the interior of the ellipse is

$$\left\{\left[\frac{(x - x_0)}{c_1}\cos\theta + \frac{(y - y_0)}{c_1}\sin\theta\right]^2 + \left[\frac{-(x - x_0)}{c_2}\sin\theta + \frac{(y - y_0)}{c_2}\cos\theta\right]^2 < 1\right\}.$$

The area of the ellipse is $\alpha = \pi c_1 c_2$, and the perimeter is $L = 4c_1E = [(c_1^2 + c_2^2)/2]^{\frac{1}{2}}2\pi$, using elliptical integral tables for E.

From Theorem II, the number N of randomly distributed ellipses intersecting a fixed ellipse has a Poisson distribution with mean

$$2\lambda c_1\left[\pi c_2 + \frac{4c_1E}{\pi}\right] \approx \pi\lambda[c_1 + c_2]^2.$$

The probability that an ellipse is isolated is

$$p_0 = \Pr(N = 0) = f(0) \approx \exp[-\pi\lambda[c_1 + c_2]^2].$$

A realization of an elliptical bombing process is shown in Fig. 10a.

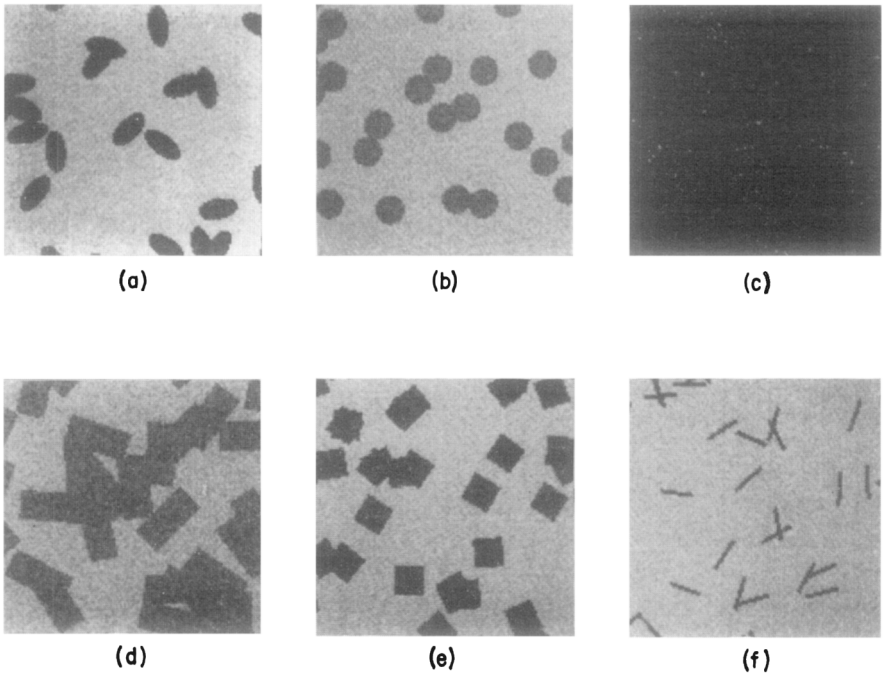

FIG. 10. Realizations of bombing processes. (a) $\mathcal{E}(25, 10/127, 5/127, 20, 10, 50, 10)$, (b) $\mathcal{C}(25, 7/127, 20, 10, 50, 10)$, (c) $\mathcal{C}(40, 1/127, 13, 10, 53, 10)$, (d) $\mathcal{R}(30, 15/127, 7/127, 20, 25, 40, 25)$, (e) $\mathcal{S}(30, 7/127, 20, 10, 50, 10)$, (f) $\mathcal{R}(30, 10/127, 1/127, 20, 10, 50, 10)$.

(*c*) *Circular Bombing Process* [18]: $\mathcal{C}[\lambda, c, \mu_1, \Sigma_1, \mu_2, \Sigma_2)$. A circular bombing process is a special case of the elliptical bombing process, where $c_1 = c_2 = c$ (Fig. 10b).

Any two circles in the plane will overlap if the distance between their centers is less than their diameter. The probability p_0 that a circle is isolated is equal to the probability that there is no circle center within radius $2r$ of a center point placed randomly on the plane. That is, $p_0 = e^{-4\pi r^2\lambda}$.

The transition probabilities for this process are given by Switzer [19]

$$p_1 P_{11}(d) = (2p_1 - 1) + (1 - p_1)^{H(d/r)}$$

where

$$H(d/r) = 1 + \left(\frac{d}{\pi r}\right)\left[1 - \left(\frac{d^2}{4r^2}\right)\right]^{\frac{1}{2}} + \left(\frac{2}{\pi}\right)\sin^{-1}\left(\frac{d}{2r}\right) \qquad \text{for } d \leq 2r$$

$$= 2 \qquad \text{for } d > 2r,$$

$$P_{12}(d) = (p_1/p_2)P_{21}(d),$$

$$P_{22}(d) = 1 - P_{12}(d),$$

$$P_{21}(d) = 1 - P_{11}(d).$$

A special case of the circular bombing process occurs when each of the circles

covers only one pixel. The process then becomes one of randomly thrown Gaussian noise (Fig. 10c).

(*d*) *Rectangular Bombing Process.* $\mathcal{R}(\lambda, c_1, c_2, \mu_1, \Sigma_1, \mu_2, \Sigma_2)$. Rectangles of major axis $2c_1$ and minor axis $2c_2$ are randomly dropped onto the plane. The orientation of a rectangle is specified by the angle θ between the x-axis and the perpendicular to the major axis of the rectangle. The midpoint of a rectangle specifies its position.

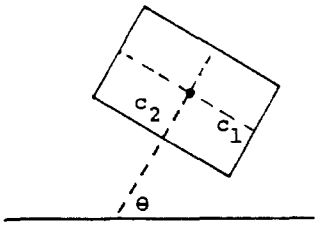

A realization of a rectangular bombing process is shown in Fig. 10d.

The equations for a rectangle are

$$|(x - x_0)\cos\theta + (y - y_0)\sin\theta| = c_1,$$
$$|-(x - x_0)\sin\theta + (y - y_0)\cos\theta| = c_2.$$

The interior of the rectangle is specified by

$$\left\{\left|\frac{(x - x_0)}{c_1}\cos\theta + \frac{(y - y_0)}{c_1}\sin\theta\right| < 1;\right.$$
$$\left.\left|\frac{-(x - x_0)}{c_2}\sin\theta + \frac{(y - y_0)}{c_2}\cos\theta\right| < 1\right\}.$$

From Theorem II, the number N of randomly distributed rectangles intersecting a fixed rectangle has a Poisson distribution with mean $8\lambda(c_1c_2 + (1/\pi)(c_1 + c_2)^2)$. The probability that a rectangle is isolated is:

$$p_0 = \Pr(N = 0) = f(0) = \exp(-8\lambda(c_1c_2 + 1/\pi(c_1 + c_2)^2)).$$

Rectangles of one pixel thickness can be used to approximate Poisson line segments (Fig. 10f).

5. STATISTICS

The statistical properties of our models can be obtained directly from the stationary and transition probabilities. We will assume that each region A_i is colored by a Gaussian random vector process having parameters μ_i and Σ_{ii}. Let

$$f(x, \mu_i, \Sigma_{ii}) = \frac{1}{(2\pi)^{q/2}|\Sigma|^{\frac{1}{2}}}\exp[-\tfrac{1}{2}(x - \mu)'\Sigma^{-1}(x - \mu)].$$

(*a*) *Histogram.* Let $H(c)$ denote the probability that a point on an image has

color c, where c is a q-element vector. For example, for visual color

$$H(c) = \Pr \begin{bmatrix} \text{red content of point } s = c_1 \\ \text{green content of point } s = c_2 \\ \text{blue content of point } s = c_3 \end{bmatrix}.$$

Then

$$H(c) = \sum_{i=1}^{m} p_i f(c, \mu_i, \Sigma_{ii}).$$

(*b*) *Co-occurrence.* Drop a Buffon needle of length d onto a picture. The endpoints of the needle are denoted by s and s'. $\Pr \begin{pmatrix} c_k \\ c_l \end{pmatrix}$ denotes the probability that s lands on color c_k and s' lands on color c_l. Then

$$\Pr \begin{pmatrix} c_k \\ c_l \end{pmatrix} = \sum_{j=1}^{m} \sum_{i=j}^{m} \Pr\,(s \in A_i, s' \in A_j) \Pr\,[\text{color}(s) = c_k \quad \text{and} \quad \text{color}(s') = c_l | s \in A_i, s' \in A_j],$$

where $\Pr\,(s \in A_i, s' \in A_j) = p_j P_{ij}(d)$, and

$$\Pr\,[\text{color}(s) = c_k, \text{color}(s') = c_l | s \in A_i, s' \in A_j] = f\left[\begin{pmatrix} c_k \\ c_l \end{pmatrix}, \begin{pmatrix} \mu_i \\ \mu_j \end{pmatrix}, \Sigma(d)\right],$$

where

$$\Sigma(d) = \begin{bmatrix} \Sigma_{ii}(0) & \Sigma_{ij}(d) \\ \Sigma_{ji}(d) & \Sigma_{jj}(0) \end{bmatrix}.$$

If there is no correlation across region boundaries, we have

$$\begin{aligned} \Pr \begin{pmatrix} c_k \\ c_l \end{pmatrix} &= \sum \sum_{i \neq j} \Pr\,(s \in A_i, s' \in A_j) \\ &\quad \times \Pr\,[\text{color}(s) = c_k, \text{color}(s') = c_l | s \in A_i, s' \in A_j] \\ &\quad + \sum_i \Pr\,(s, s' \in A_i) \Pr\,[\text{color}(s) = c_k, \text{color}(s') = c_l | s, s' \in A_i] \\ &= \sum_{i \neq j} p_j P_{ij}(d) f\left[\begin{pmatrix} c_k \\ c_l \end{pmatrix}, \begin{pmatrix} \mu_i \\ \mu_j \end{pmatrix}, \hat{\Sigma}(d)\right] + \sum_i p_i P_{ii}(d) f\left[\begin{pmatrix} c_k \\ c_l \end{pmatrix}, \begin{pmatrix} \mu_i \\ \mu_i \end{pmatrix}, \Sigma(d)\right], \end{aligned}$$

where

$$\hat{\Sigma}(d) = \begin{bmatrix} \Sigma_{ii}(0) & 0 \\ 0 & \Sigma_{jj}(0) \end{bmatrix}.$$

In the cell structure models discussed in Section 3, where it is assumed that cells are independently colored, we have no correlation across cell boundaries, and we

obtain

$$\Pr\begin{pmatrix} c_k \\ c_l \end{pmatrix} = \sum_{i \neq j} p_j P_{ij}(d) f\left[\begin{pmatrix} c_k \\ c_l \end{pmatrix}, \begin{pmatrix} \mu_i \\ \mu_j \end{pmatrix}, \hat{\Sigma}(d)\right] + \sum_i p_i^2 (1 - W(d)) f\left[\begin{pmatrix} c_k \\ c_l \end{pmatrix}, \begin{pmatrix} \mu_i \\ \mu_i \end{pmatrix}, \hat{\Sigma}(d)\right] + \sum_i p_i W(d) f\left[\begin{pmatrix} c_k \\ c_l \end{pmatrix}, \begin{pmatrix} \mu_i \\ \mu_i \end{pmatrix}, \Sigma(d)\right].$$

(*c*) *Difference.* Again drop a needle of length d onto a picture. Let $\mathfrak{D}(\Delta)$ denote the sum over all colors c of the probability that s' lands on color $c + \Delta$ and s lands on color c. Then

$$\mathfrak{D}(\Delta) = \sum_i \sum_j \int_c \Pr(s \in A_i, s' \in A_j) \Pr[\text{color}(s) = c, \text{color}(s') = c + \Delta \mid s \in A_i, s' \in A_j)].$$

The equations under various assumptions are analogous to those for co-occurrence.

(*d*) *Variogram.* Again drop a needle of length d onto a picture. Let $V(d)$ denote the mean squared color difference at the endpoints of the needle. Then

$$V(d) = E[(\text{color}(s) - \text{color}(s'))^t(\text{color}(s) - \text{color}(s'))].$$

If there is no correlation across region boundaries we get

$$V(d) = \sum_i \sum_j [\Sigma_{ii}(d) + \Sigma_{jj}(d) + (\mu_i - \mu_j)^t(\mu_i - \mu_j)]p_j P_{ij}(d)$$

For the cell structure models, there is no correlation across cell boundaries, and we have

$$V(d) = \sum \sum_{i \neq j} [\Sigma_{ii}(0) + \Sigma_{jj}(0) + (\mu_i - \mu_j)^t(\mu_j - \mu_j)]p_j P_{ij}(d) + \sum_i [2\Sigma_{ii}(d)]p_i W(d) + \sum_i [2\Sigma_{ii}(0)]p_i^2[1 - W(d)].$$

(*e*) *Autocorrelation.* We will use the definition of the autocovariance function $AC(d)$ to derive the autocorrelation function $\rho(d)$ for a gray level mosaic texture [20]:

$$AC(d) = \sum_i p_i g_i (\sum_j P_{ji}(d) g_j) - g^2,$$

where g_i denotes the mean gray level of the type-i cell, $g = \sum_i p_i g_i$ is the expected gray level of a randomly selected point, and the gray levels within a cell are assumed to be uncorrelated.

The autocorrelation function can be written as

$$\rho(d) = \frac{AC(d)}{AC(0)} = \frac{AC(d)}{\sigma^2}.$$

We can write the autocorrelation in terms of the transition probabilities as

$$\rho(d) = \frac{1}{\sigma^2}\left[\sum_i p_i g_i \left(\sum_j P_{ji}(d) g_j\right) - g^2\right]$$

$$= \frac{1}{\sigma^2}\left[\sum_i p_i g_i \left(\sum_{j \neq i} P_{ji}(d) g_j + P_{ii}(d) g_i\right) - g^2\right]$$

$$= \frac{1}{\sigma^2}\left[\sum_i p_i g_i \left(\sum_{j \neq i} p_j g_j - W(d) \sum_{j \neq i} p_j g_j + p_i g_i + W(d) g_i - W(d) p_i g_i\right) - g^2\right]$$

$$= \frac{1}{\sigma^2}\left[\sum_i p_i g_i (g\bar{W}(d) + g_i W(d)) - g^2\right]$$

$$= \frac{1}{\sigma^2}\left[g^2 \bar{W}(d) + W(d) E(g_i^2) - g^2\right] = \frac{1}{\sigma^2}\left[E(g_i^2) - g^2\right] W(d)$$

$$= \frac{\sigma^2}{\sigma^2} W(d) = W(d).$$

In the above, $\bar{W}(d) = 1 - W(d)$.

6. DISCUSSION

We will list some properties of mosaic models that may be potential advantages if they are used in image modeling. A detailed discussion of these properties can be found in [20].

(1) Mosaic models describe images by specifying geometrical processes that may have generated the visual pattern under consideration. Such a constructive description, therefore, inherently encompasses the specification of all the information about the pattern. One may extract from the model as much information as desired, e.g., autocorrelation properties which may not be unique to the image. For example, characterization of a pattern in terms of its autocorrelation properties ignores any phase information.

(2) Mosaic models do not simply involve capturing the dependence of a certain local feature on a certain neighborhood. There is no assumption about the Markovianity of the data.

(3) The task of modeling a variety of images is divided between the steps of model selection and parameter specification.

(4) The underlying idea of treating the image as an arrangement of regions provides a hierarchical character to the mosaic models, which may be useful due to the similar nature of many real images.

(5) Mosaic models seem intuitively meaningful. A pattern corresponding to a specified model, and the implications of the variations in parameter values, are relatively easy to visualize.

Several properties of the models that could prove to be useful for model-fitting are suggested in [20]. Some of the models have been analyzed with respect to several of these properties. References [22, 23] present a general method of obtaining the expected number and expected perimeter of the connected com-

ponents obtained by randomly coloring points in various lattices, and relates these properties of the lattices to the corresponding properties of the connected components formed in cell structure mosaics. Reference [24] presents a method of obtaining the expected perimeter and the expected covered area in patterns formed by general, multicolored bombing models using convex bombs under certain orientation constraints. Reference [25] presents a method of estimating the expected number of connected components in bombing patterns. A discussion of texture measures can be found in [21]. In a forthcoming paper [26], estimates of the autocorrelation properties of the various mosaic models are provided. Work is under way to apply the available knowledge about these models to the modeling of various classes of images.

REFERENCES

1. B. Mandelbrot, "Fractals—Form, Chance, and Dimension," Freeman, San Francisco, 1977.
2. E. Wong, Two-dimensional random fields and representations of images, *SIAM J. Appl. Math.* **16**(4), 1968, 756–770.
3. M. Hassner, Markov models of digitized images—A data compression analysis, submitted.
4. G. Matheron, The theory of regionalized variables and its applications, *Les Cahiers du Centre de Morphologie Math. de Fontainbleau* **5**, 1971.
5. B. H. McCormick and S. N. Jayaramamurthy, Time series model for texture synthesis, *Int. J. Computer and Information Sciences* **3**, 1974, 329–343.
6. B. Ripley, Modelling spatial patterns, *J. Royal Stat. Soc.* **8**, 1977, 172–212.
7. B. Matern, *Spatial Variation,* Medd Statens Skogsforskningsinstitut, Stockholm, 36(5), 1–144, 1960.
8. B. Matern, Doubly stochastic Poisson processes in the plane, *in Statistical Ecology,* Vol. 1, pp. 195–213, Univ. of Pennsylvania Press, 1971.
9. B. Ripley, "Stochastic Geometry and the Analysis of Spatial Pattern," Ph.D. thesis, Cambridge University, May 1976.
10. M. S. Bartlett, "The Statistical Analysis of Spatial Pattern," Wiley, New York, 1975.
11. E. Pielou, "An Introduction to Mathematical Ecology," Wiley, New York 1977.
12. P. Switzer, A random set process in the plane with a Markovian property, *Ann. Math. Stat.* **36**, 1965, 1859–1863.
13. R. Miles, On the homogeneous planar Poisson point-process, *Math. Biosciences* **6**, 1970, 85–127.
14. E. Gilbert, Random subdivisions of space into crystals, *Ann. Math. Stat.* **33**, 1962, 958–972.
15. D. Thompson, "On Growth and Form," Vol. II, Cambridge Univ. Press, London, 1963.
16. L. Santaló, *Encyclopedia of Mathematics and its Applications,* Vol. 1: *Integral Geometry and Geometric Probability,* Addison–Wesley, Reading, Mass., 1976.
17. D. Dufour, "Intersections of Random Convex Regions," Stanford University, Dept. of Statistics, T. R. 202, 1973.
18. S. Roach, "The Theory of Random Clumping," Methuen, London, 1968.
19. P. Switzer, Reconstructing patterns from sample data, *Ann. Math. Stat.* **38**, 1967, 138–154.
20. N. Ahuja, "Mosaic Models for Image Analysis and Synthesis," University of Maryland, Computer Science Center, T.R. 607, November 1977.
21. B. Schachter, Texture measures, to be published.
22. N. Ahuja, "Connectivity in Lattices and Mosaics," University of Maryland, Computer Science Center, T.R. 637, February 1978.
23. N. Ahuja, "Connectivity in Lattices and Mosaics, II," University of Maryland, Computer Science Center, T.R. 671, June 1978.
24. N. Ahuja, "Geometrical Properties of Bombing Patterns," University of Maryland Computer Science Center, T.R. 673, June 1978.
25. N. Ahuja, "Connectedness Properties of Bombing Patterns," University of Maryland Computer Science Center, T.R. 682, July 1978.
26. N. Ahuja, "Autocorrelation in Mosaics," University of Maryland, Computer Science Center, T.R. 695, September 1978.